JOURNAL OF PROPULSION AND POWER
Vol. 18, No. 3, May–June 2002

Unsteady Cascade Aerodynamics in the Time Domain

Dana A. Gottfried* and Sanford Fleeter†
Purdue University, West Lafayette, Indiana 47907

A linearized unsteady incompressible aerodynamic model for airfoil cascades is developed that is not restricted to harmonic motion at a constant interblade phase angle. This is accomplished by starting with the unsteady aerodynamic coefficients generated by LINSUB, a semianalytic unsteady cascade aerodynamics code that assumes linearity in both space and time. An inverse Fourier transform is then performed to predict the unsteady aerodynamic forces on the airfoils due to an impulsive acceleration. This result, termed the cascade indicial function, is then convolved with the arbitrary motion of the blades to obtain the unsteady aerodynamic forces on the airfoils in the time domain. The aerodynamic damping predicted by the time domain model is shown to compare well to LINSUB results when the interblade phase angle is constant. Results demonstrating the ability of the model to handle arbitrary airfoil motion are also presented.

Nomenclature

B	=	number of blades
C_x	=	aerodynamic coefficient
c	=	blade chord
$\overline{\text{c.g.}}$	=	center of gravity location (zero at leading edge)
d	=	$\overline{\text{c.g.}} - \overline{\text{e.a.}}$
$\overline{\text{e.a.}}$	=	elastic axis location (zero at leading edge)
F	=	Fourier transform operator
h	=	bending amplitude
$\bar{h}(t)$	=	step function, 0 for $t < 0$, 1 for $t \geq 0$
I	=	number of poles
I_G	=	moment of inertia of blade about $\overline{\text{c.g.}}$ per unit span
j	=	$\sqrt{-1}$
K_h	=	bending stiffness of blade per unit span
K_α	=	torsion stiffness of blade per unit span
k	=	reduced frequency, $\omega c/U$
$L(t)$	=	lift in time due to bending and pitching
$M(t)$	=	moment in time due to bending and pitching
$\bar{M}_x$	=	cascade indicial function
m	=	location index of the airfoil in the cascade
$\bar{m}$	=	mass of blade per unit span
$r(t)$	=	ramp function, 0 for $t < 0$, t for $t \geq 0$
t	=	time
U	=	steady-state flow velocity
α	=	pitching amplitude
α, ν, μ	=	curve fit constants for indicial functions
β	=	interblade phase angle
$\delta(t)$	=	delta function, 1 at $t = 0$, 0 elsewhere
ρ	=	steady-state flow density
τ	=	exponential decay time constant, dummy integration variable

Subscripts

h	=	bending
L	=	lift
M	=	moment
α	=	pitching

Superscript

$*$	=	complex conjugate

Received 20 July 2001; revision received 17 December 2001; accepted for publication 17 December 2001.

*Postdoctoral Researcher, School of Mechanical Engineering, 1003 Chaffee Hall; gottfrie@purdue.edu. Member AIAA.

†McAllister Distinguished Professor, School of Mechanical Engineering, 1003 Chaffee Hall; fleeter@purdue.edu. Fellow AIAA.

Introduction

UNSTEADY aerodynamic phenomena continue to produce serious aeroelastic problems in the development of new multistage turbomachinery. Two families of computational techniques are currently available to address these problems. The most widely used are the time-marching techniques. In these, the fluid equations (e.g., the potential, Euler, or Navier–Stokes equations) are marched in time from one time level to the next, simulating the flow through the turbomachine. This approach, although very powerful and quite general, is computationally very expensive, resulting in these codes being prohibitively expensive for design use.

The second family of techniques are the time-linearized analysis techniques. The time averaged steady flow through the turbomachine is first solved using the nonlinear governing fluid equations. The governing equations are then linearized, which is accomplished by assuming that the unsteadiness in the flow is small compared to the mean flow. The resulting small disturbance equations are then solved, under the assumption that the disturbance flow is harmonic in time. The advantage of the time-linearized approach is that it is computationally very efficient, typically reducing computational time by several orders of magnitude compared to the time-marching approach. Thus, these time-linearized codes form the basis of design analyses.

In the category of time-linearized techniques, LINSUB[1] is a widely used and generally available code for stability and forced-response analyses in turbomachines. LINSUB uses a semianalytical approach to model an infinite, two-dimensional cascade of flat plates with zero mean incidence represented by singularity distributions. The flat plate assumption means the model is not only linear in time, but also in space. LINFLO[2] is another time-linearized code, but it does not assume linearity in space so that it can model airfoil thickness effects. Both LINSUB and LINFLO provide a quick way to determine whether or not a given design will be flutter free or will minimize stresses due to external aerodynamic forcing mechanisms.

Unfortunately, the basic assumptions inherent in time-linearized analyses are too restrictive for some applications. Specifically, time-linearized analyses assume that all of the blades in a cascade oscillate with harmonic time dependence at a specific frequency and with a constant phase relationship between blades. However, there are many situations where the blades may not be oscillating harmonically and with a constant interblade phase angle, rendering time-linearized codes unable to be applied directly. For example, if there are material differences from blade-to-blade, that is, mistuning, the frequency of oscillation will not be the same for all blades.

These restrictions can be removed and the application of these time-linearized analyses extended. This requires the development of appropriate postprocessing analyses. Namely, the time-linearized theory predicted unsteady aerodynamic coefficients must be generated over a range of frequencies and these results then transformed back to the time domain. The restriction of constant interblade phase angle can be removed by performing a discrete transform over all interblade phase angles. Mengle[3] considered these transforms for the bending lift coefficient and built a solid foundation for the technique. To make the method more generally applicable, the pitching moment and the aerodynamic coupling between bending and pitching must also be considered.

This paper describes an incompressible unsteady aerodynamic model for cascades that is not restricted to harmonic motion with a constant interblade phase angle. The model starts with the unsteady aerodynamic lift coefficients due to bending, moment coefficients due to pitching, and the coupling coefficients (i.e., lift due to pitching and moment due to bending) predicted by LINSUB. An inverse Fourier transform is performed to predict the aerodynamic forces due to an impulsive acceleration. This cascade indicial function is then convolved with the arbitrary motion of the airfoils to obtain the aerodynamic force in the time domain. The analysis is utilized to demonstrate the unsteady aerodynamics of a cascade undergoing arbitrary blade motion.

Unsteady Aerodynamic Coefficients

The LINSUB aerodynamic model provides unsteady aerodynamic coefficients at a given frequency and interblade phase angle. These complex coefficients include 1) lift due to bending C_{Lh}, 2) lift due to pitching $C_{L\alpha}$, 3) moment due to bending C_{Mh}, and 4) moment due to pitching $C_{M\alpha}$. Whenever appropriate, the symbol C_x will be used to represent these four aerodynamic coefficients. The bending coefficients are due to a specified motion of the airfoils of the form $\dot{h}_m = \dot{h}_0 \exp[j(kt + m\beta)]$, where the dot denotes differentiation with respect to time. The pitching coefficients are due to a specified motion of the airfoils of the form $\alpha_m = \alpha_0 \exp[j(kt + m\beta)]$. The aerodynamic lift $L_m(t)$ and moment $M_m(t)$ on blade m are $C_{Lh}\dot{h}_m + C_{L\alpha}\alpha_m$ and $C_{Mh}\dot{h}_m + C_{M\alpha}\alpha_m$, respectively.

Negative Frequencies

The approach to transforming the LINSUB unsteady aerodynamic coefficients to the time domain involves the inverse Fourier transform. Because the inverse Fourier transform requires integration over the entire real frequency axis, negative frequencies must be considered. These have no direct physical meaning, but exist mathematically. The following provides some physical insight in to the use of negative frequencies in later sections dealing with the inverse Fourier transform.

The aerodynamic coefficient $C_x(k, \beta)$ is found for a given airfoil boundary condition of the form $X \exp[j(kt + m\beta)]$. Here X is the amplitude of the airfoil motion, equal to $\dot{h}_0$ for bending and α_0 for pitching. Consider what happens if the sign of both k and β are changed. The real part of the velocity boundary condition will remain the same and the imaginary part will change signs. Because the LINSUB analysis is linear, any change of signs in the boundary conditions will cause a change of signs in the result. Hence,

$$\mathrm{Re}\{C_x(k, \beta)\} = \mathrm{Re}\{C_x(-k, -\beta)\} \tag{1}$$

$$\mathrm{Im}\{C_x(k, \beta)\} = -\mathrm{Im}\{C_x(-k, -\beta)\} \tag{2}$$

or

$$C_x(k, \beta) = C_x^*(-k, -\beta) \tag{3}$$

Thus, a positive frequency condition such as $C_x(k, -\beta)$ can be related to the negative frequency condition $C_x(-k, \beta)$:

$$C_x(k, -\beta) = C_x^*(-k, \beta) \tag{4}$$

Note that for quasi-steady motion, that is, $k \to 0$, and zero interblade phase angle this implies that the imaginary part of the lift is zero. This means the lift is in phase or antiphase with the airfoil motion. This will not be true for $k \to 0$ with $\beta \neq 0$ because the out-of-phase motion of adjacent airfoils will produce some lift on the reference airfoil even if its velocity is zero.

Cascade Indicial Functions

The convolution integral is a convenient solution technique for linear system forced response. For a linear spring–mass system having an externally applied force $f(t)$, the convolution solution is

$$x(t) = \int_0^t \hat{h}(t - \tau) f(\tau)\, \mathrm{d}\tau \tag{5}$$

where $\hat{h}(t)$ is the characteristic response of the system to a unit impulse applied at $t = 0$.

For the unsteady aerodynamic problem being considered here, a key step is to find the characteristic function analogous to $\hat{h}(t)$. This function is called the cascade indicial function and is given as $\bar{M}_x(t, \beta)$. The subscript x represents the four different indicial functions, one for each aerodynamic coefficient.

For the linearized unsteady cascade model, there is no explicit external force applied. Rather, the motion of the airfoils is specified at some constant frequency. Thus, instead of dealing with an impulsive force, an impulsive acceleration of the airfoils is considered. The cascade indicial function represents the unsteady aerodynamic lift/moment acting on the airfoils when they experience this impulsive acceleration. The impulsive accelerations take the following forms. The bending coefficients are

$$\ddot{h}_m = \delta(t) e^{jm\beta} \tag{6}$$

The pitching coefficients are

$$\ddot{\alpha}_m = \delta(t) e^{jm\beta} \tag{7}$$

Note that the impulsive acceleration depends on the interblade phase angle. Thus, there will be as many indicial functions as there are interblade phase angles.

The lift/moment acting on airfoil m due to this impulse is $\bar{M}_x(t, \beta) e^{jm\beta}$. The interblade phase angle β appears both implicitly in the indicial function and explicitly in the $e^{jm\beta}$ term. The implicit dependence occurs because the motion of the cascade, taken as a whole, affects the unsteady aerodynamics. In addition, the linearity of the problem requires that the airfoil-to-airfoil variation represented by the $e^{jm\beta}$ term in the boundary conditions must also be present in the airfoil-to-airfoil variation of the lift/moment.

Once $\bar{M}_x(t, \beta)$ is found, it can be convolved with any arbitrary acceleration of the cascade airfoils (at a specific interblade phase angle) to find the aerodynamic lift/moment on the airfoils. By analogy with Eq. (5), the lift and moment are

$$L_m(t) = \int_0^t \bar{M}_{Lh}(t - \tau, \beta) e^{jm\beta} \ddot{h}_m(\tau)\, \mathrm{d}\tau + \int_0^t \bar{M}_{L\alpha}(t - \tau, \beta) e^{jm\beta} \ddot{\alpha}_m(\tau)\, \mathrm{d}\tau \tag{8}$$

$$M_m(t) = \int_0^t \bar{M}_{Mh}(t - \tau, \beta) e^{jm\beta} \ddot{h}_m(\tau)\, \mathrm{d}\tau + \int_0^t \bar{M}_{M\alpha}(t - \tau, \beta) e^{jm\beta} \ddot{\alpha}_m(\tau)\, \mathrm{d}\tau \tag{9}$$

To this point, the analysis is restricted to airfoil motion at a specific interblade phase angle. However, this restriction will be removed at a later point in this analysis.

Derivation via Fourier Transforms

Next consider how to use Fourier transforms of the LINSUB coefficients to obtain the cascade indicial functions. The Fourier transform is denoted by F. Functions in the time domain are given lowercase letters, whereas their associated Fourier transforms are

given uppercase letters. For a function $g(t)$, the Fourier transform and inverse Fourier transform are defined as

$$F[g(t)] = G(k) = \int_{-\infty}^{\infty} g(t)e^{-jkt}\,dt \tag{10}$$

$$F^{-1}[G(k)] = g(t) = \frac{1}{2\pi}\int_{-\infty}^{\infty} G(k)e^{jkt}\,dk \tag{11}$$

where k is the Fourier transform variable.

Consider an ordinary differential equation that describes some physical process:

$$L[x(t)] = g(t) \tag{12}$$

where L is a linear operator, $x(t)$ is the dependent variable, and $g(t)$ is the external forcing.

Take the Fourier transform of this equation to obtain

$$L(k)X(k) = G(k) \tag{13}$$

$L(k)$ is the Fourier transform representation of the linear operator L. In transform space, the operator becomes an algebraic coefficient. The solution $X(k)$ in transform space is simply $G(k)/L(k)$. An inverse Fourier transform is performed to revert to the time domain:

$$x(t) = \frac{1}{2\pi}\int_{-\infty}^{\infty} \frac{G(k)}{L(k)}e^{jkt}\,dk \tag{14}$$

Consider $g(t) = e^{jk_0t}$, which corresponds to simple harmonic forcing at the frequency k_0. The Fourier transform of $g(t) = e^{jk_0t}$ is just $2\pi\delta(k_0 - k)$. Substitute this into Eq. (14),

$$x(t) = \frac{1}{2\pi}\int_{-\infty}^{\infty} \frac{2\pi\delta(k_0 - k)}{L(k)}e^{jkt}\,dk = \frac{1}{L(k_0)}e^{jk_0t} \tag{15}$$

From this, an important analogy is drawn to the LINSUB aerodynamic coefficients. In LINSUB, the unsteady aerodynamic coefficients are found when the airfoil is forced at a single frequency. The time dependence of this harmonic forcing is dropped from the problem during the analysis. To regain the time dependence, the LINSUB coefficients must be multiplied by e^{jk_0t}. Thus, it is deduced that the $1/L(k)$ term in Eq. (15) is analogous to the unsteady aerodynamic coefficients calculated by LINSUB: $C_x(k, \beta) \sim 1/L(k)$. Thus, to generally transform the LINSUB frequency-domain results back to the time domain, take the inverse Fourier transform of the unsteady aerodynamic coefficient multiplied by the Fourier transform of its associated forcing. This forcing is the bending velocity for the bending coefficients and the pitching displacement for pitching coefficients. For example, the moment due to pitching in the time domain is

$$M(t) = \frac{1}{2\pi}\int_{-\infty}^{\infty} C_{M\alpha}(k, \beta)G(k)e^{jkt}\,dk \tag{16}$$

Here $G(k)$ is the Fourier transform of the pitching displacement of the airfoil. In the simple case of forcing at single frequency k_0, $G(k) = 2\pi\delta(k_0 - k)$, and Eq. (16) is easily evaluated to give $M(t) = C_{M\alpha}(k_0, \beta)e^{jk_0t}$.

The cascade indicial function $\bar{M}_x(t, \beta)$ is the unsteady aerodynamic force acting on the airfoil cascade when it is subjected to an impulsive pitching or bending acceleration having interblade phase angle β. For the bending problem, the applied boundary condition in LINSUB is the bending velocity. An applied bending acceleration impulse causes the bending velocity to behave as a step function. The Fourier transform of the step function is $1/jk$. Thus, the cascade indicial function for bending is

$$\bar{M}_{xh}(t, \beta) = \frac{1}{2\pi}\int_{-\infty}^{\infty} \frac{C_{xh}(k, \beta)}{jk}e^{jkt}\,dk \tag{17}$$

where the x subscript can represent either lift L or moment M.

The singularity at $k = 0$ can be removed by adding and subtracting the appropriate term:

$$\bar{M}_{xh}(t, \beta) = \frac{1}{2\pi}\int_{-\infty}^{\infty} \frac{C_{xh}(0, \beta)}{jk}e^{jkt}\,dk + \frac{1}{2\pi}\int_{-\infty}^{\infty} \frac{C_{xh}(k, \beta) - C_{xh}(0, \beta)}{jk}e^{jkt}\,dk \tag{18}$$

Recalling that the Fourier transform of the step function is $1/jk$, the first term can be simplified:

$$\bar{M}_{xh}(t, \beta) = C_{xh}(0, \beta)\bar{h}(t) + \frac{1}{2\pi}\int_{-\infty}^{\infty} \frac{C_{xh}(k, \beta) - C_{xh}(0, \beta)}{jk}e^{jkt}\,dk \tag{19}$$

For the pitching problem, the applied boundary condition in LINSUB is the angular displacement. An impulsive pitching acceleration causes the angular displacement to behave as the ramp function. (The ramp function is 0 for $t < 0$, and t for $t \geq 0$). The Fourier transform of the ramp function is $-1/k^2$. Thus, the cascade indicial function for pitching is

$$\bar{M}_{x\alpha}(t, \beta) = \frac{-1}{2\pi}\int_{-\infty}^{\infty} \frac{C_{x\alpha}(k, \beta)}{jk}e^{jkt}\,dk \tag{20}$$

The singularity at $k = 0$ can be removed by adding and subtracting the appropriate term:

$$\bar{M}_{x\alpha}(t, \beta) = \frac{-1}{2\pi}\int_{-\infty}^{\infty} \frac{C_{x\alpha}(0, \beta)}{k^2}e^{jkt}\,dk + \frac{-1}{2\pi}\int_{-\infty}^{\infty} \frac{C_{x\alpha}(k, \beta) - C_{x\alpha}(0, \beta)}{k^2}e^{jkt}\,dk \tag{21}$$

When it is recalled that the Fourier transform of the ramp function is $-1/k^2$, the first term can be simplified:

$$\bar{M}_{x\alpha}(t, \beta) = C_{x\alpha}(0, \beta)r(t) + \frac{-1}{2\pi}\int_{-\infty}^{\infty} \frac{C_{x\alpha}(k, \beta) - C_{x\alpha}(0, \beta)}{k^2}e^{jkt}\,dk \tag{22}$$

Once the coefficients from LINSUB are obtained, for both negative and positive frequencies, a numeric integration scheme is used to evaluate the integrals in Eqs. (19) and (22).

Numeric Integration Scheme

The approach taken is to approximate the variation of the LINSUB coefficients in the frequency domain with an analytic expression that can be easily inverted.

Bending Coefficients

Mengle[3] investigated the exact form of the analytic expression that is most appropriate for bending coefficients. He found that an appropriate analytic expression is

$$C_{xh}(k, \beta) = \alpha_0 + j\nu_0 + \sum_{i=1}^{I} \frac{(\alpha_i + j\nu_i)jk}{jk + \mu_i} + (\alpha_{I+1} + j\nu_{I+1})jk \tag{23}$$

The α, ν, and μ coefficients are found by plotting the LINSUB coefficients vs reduced frequency and performing a least-squares curve fit. Although not explicitly shown, the α, ν, and μ coefficients are functions of the interblade phase angle β because a curve fit is performed for each possible interblade phase angle.

Substituting Eq. (23) into Eq. (19) gives

$$\bar{M}_{xh}(t, \beta) = (\alpha_0 + j\nu_0)\bar{h}(t) + \frac{1}{2\pi}\int_{-\infty}^{\infty} \left\{ \sum_{i=1}^{I} \left[\frac{(\alpha_i + j\nu_i)jk}{jk + \mu_i} \right] + \alpha_{I+1} + j\nu_{I+1} \right\} e^{jkt}\,dk \tag{24}$$

This is simplified using the Fourier transform of the delta function and the theory of residues:

$$\bar{M}_{xh}(t,\beta) = (\alpha_0 + j\nu_0)\bar{h}(t) + \sum_{i=1}^{I}(\alpha_i + j\nu_i)e^{-\mu_i t} + (\alpha_{I+1} + j\nu_{I+1})\delta(t) \tag{25}$$

At this point, note the physical meaning of these terms. Recall that to find the force or moment the indicial function must be shifted in time, multiplied by the bending acceleration, and integrated. Thus, the constant term $\alpha_0 + j\nu_0$ becomes a factor multiplying the bending velocity. Physically, it represents the quasi-steady part of the aerodynamics. The term multiplying the delta function $\alpha_{I+1} + j\nu_{I+1}$ becomes a coefficient for the bending acceleration. It represents the added-mass effect. The middle terms, which include the $\alpha_i + j\nu_i$ coefficients and the decay constants μ_i, take into account the fully unsteady effects caused by the vortices being shed by the airfoils and propagating downstream. It will be seen that these fully unsteady terms are the most time consuming to evaluate because they require the calculation of a convolution integral at each time step.

Pitching Coefficients

An analytic expression appropriate for approximating the pitching coefficients will not be the same as that for bending. For the bending problem, LINSUB takes the velocity of the airfoils as the boundary condition, whereas for the pitching problem, the angular displacement is taken. This is an important distinction. For a given harmonic angular acceleration at frequency k, the corresponding angular displacement will be proportional to k^2. Thus, the analytic expression for the lift/moment coefficients must contain a k^2 term. It should also contain all of the lower powers of k. Given this, the following expression was found to be appropriate:

$$C_{x\alpha}(k,\beta) = \alpha_0 + j\nu_0 - \sum_{i=1}^{I}\frac{(\alpha_i + j\nu_i)k^2}{jk + \mu_i} + (\alpha_{I+1} + j\nu_{I+1})jk - (\alpha_{I+2} + j\nu_{I+2})k^2 \tag{26}$$

Substituting this into Eq. (22) gives

$$\bar{M}_{x\alpha}(t,\beta) = (\alpha_0 + j\nu_0)r(t) + \frac{1}{2\pi}\int_{-\infty}^{\infty}\left\{\sum_{i=1}^{I}\left[\frac{(\alpha_i + j\nu_i)jk}{jk + \mu_i}\right] + \frac{\alpha_{I+1} + j\nu_{I+1}}{jk} + \alpha_{I+2} + j\nu_{I+2}\right\}e^{jkt}\,\mathrm{d}k \tag{27}$$

As before, the expression under the integral can be evaluated using residue theory:

$$\bar{M}_{x\alpha}(t,\beta) = (\alpha_0 + j\nu_0)r(t) + \sum_{i=1}^{I}(\alpha_i + j\nu_i)e^{-\mu_i t} + (\alpha_{I+1} + j\nu_{I+1})\bar{h}(t) + (\alpha_{I+2} + j\nu_{I+2})\delta(t) \tag{28}$$

The physical meanings of the terms is as follows. The first term is a quasi-steady term proportional to the angular displacement. The second term is the fully unsteady term, taking into account the effect of the shed vortices. The third term is another quasi-steady term proportional to the angular velocity, and the fourth term is the added-mass effect.

At this point, the indicial functions have been found in terms of the α, ν, and μ coefficients in Eqs. (25) and (28). With the indicial function in this form, the convolution integrals of Eqs. (8) and (9) can be readily evaluated. However, before this is done, consider how to obtain the α, ν, and μ coefficients from the LINSUB result.

Least-Squares Fit

A table of LINSUB aerodynamic coefficients vs k over the range $-10 < k < 10$ is first generated. The reduced frequency can be confined to $-10 < k < 10$ because at high reduced frequencies the added-mass effect dominates the lift and moment. The added-mass effect is, by definition, proportional to the acceleration of the airfoil and is mathematically taken into account with the jk term for bending and the k^2 for pitching in Eqs. (23) and (26), respectively.

The α, ν, and μ coefficients in Eqs. (23) and (26) are found by performing a least-squares fit on the LINSUB data. Following the lead of Mengle,[3] the least-squares algorithm is made linear by making μ an input parameter. A FORTRAN program begins a cycle of finding the least-squares fit starting from this value, finding its associated error, and incrementing μ accordingly. The cycle continues until the error is minimized. The number of terms I needed for the fully unsteady part is 1–3 for most practical problems. Mengle has shown that $I = 1$ is appropriate for many problems. He also observed the trend that as the spacing-to-chord ratio is increased more terms are needed.

Removing the Interblade Phase Restriction

In certain situations the airfoils will not move at a constant interblade phase angle with respect to one another. For example, slight material differences from airfoil to airfoil and inlet distortions can produce vibrations within the blade row that have no interblade phase relationship. Furthermore, a part-span shroud will couple the airfoils and cause them to vibrate in modal patterns that have no interblade phase relationship. Fortunately, the linearity of the LINSUB analysis enables the solutions to be superimposed in such a way that the interblade phase angle restriction is removed.

For illustration purposes, consider a four-bladed rotor at zero stagger with one blade executing a bending vibration and all others stationary. The rotor unwrapped on a two-dimensional plane is shown on the left-hand side of Fig. 1. Because it is a rotor, it is periodic, and the blade above $m = 3$ is the same as blade $m = 0$. Small arrows represent the bending velocity, and dashed lines represent the blades at maximum displacement.

Summing the four situations shown in the right-hand side of Fig. 1 and dividing by four duplicates this situation. That is, the right-hand side boundary conditions sum to equal the left-hand side boundary condition. Therefore, because the problem is linear, the solutions for each case on the right-hand side can be summed to obtain the solution to the problem of only blade $m = 0$ moving.

Now that a physical understanding has been gained, consider the fundamental mathematical principle involved. For any complex number x raised to the power l,

$$\sum_{l=1}^{B} x^l = \begin{cases} x\dfrac{1-x^B}{1-x} & \text{if} \quad x \neq 1 \\ B & \text{if} \quad x = 1 \end{cases} \tag{29}$$

Substitute $x = \exp(jm2\pi/B)$, then for m, strictly an integer,

$$\frac{1}{B}\sum_{l=1}^{B}\exp(jm2\pi/B) = \begin{cases} 0 & \text{if} \quad m \neq 0, B, 2B, \ldots \\ 1 & \text{if} \quad m = 0, B, 2B, \ldots \end{cases} \tag{30}$$

The imposed motion of the blades in LINSUB takes into account the interblade phase by the term $e^{jm\beta}$. The rotor must be periodic over its B blades, and so the only possible interblade phase angles are

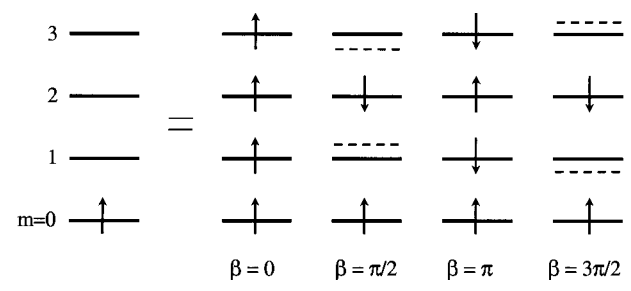

Fig. 1 One blade executing harmonic motion and equivalent representation.

$$\beta_l = 2\pi l/B, \qquad \ell = 1, 2, \ldots, B \tag{31}$$

Thus, when the blade motions represented by all possible interblade phase angles are summed and divided by the number of blades, the result is that just blade $m = 0$ will move, with all of the other blades being stationary. Therefore, Eq. (30) is a mathematical statement of the qualitative argument made with Fig. 1.

Aerodynamic coefficients can be obtained from LINSUB for each possible interblade phase angle and, because the problem is linear, these can be summed to obtain the solution to the problem of only the $m = 0$ blade moving. Furthermore, the cascade indicial functions are linearly related to the aerodynamic coefficients via an inverse Fourier transform. Therefore, the indicial functions for each interblade phase angle can be summed to obtain the lift/moment on blade m due to blade 0 being impulsively accelerated. Call this lift/moment $\Pi_{m,0}$:

$$\Pi_{m,0} = \frac{1}{B}\sum_{l=1}^{B} \bar{M}_x(t, \beta_l) e^{jm\beta_l} \tag{32}$$

As expected, even though blade $m = 0$ is the only blade impulsively started, it is possible for the other blades to experience a nonzero lift/moment.

Equation (30) can be made more general so that it handles the case of a blade other than $m = 0$ being impulsively accelerated. The parameter m must be replaced by $p - n$:

$$\frac{1}{B}\sum_{l=1}^{B} \exp[j(p-n)2\pi l/B] = \begin{cases} 0 & \text{if} \quad p-n \neq 0, B, 2B, \ldots \\ 1 & \text{if} \quad p-n = 0, B, 2B, \ldots \end{cases} \tag{33}$$

The parameter p is the number of the blade that is impulsively accelerated, and n is the appropriate phase shift parameter. Then the resulting lift/moment is

$$\Pi_{p,n} = \frac{1}{B}\sum_{l=1}^{B} \bar{M}_x(t, \beta_l) \exp[j(p-n)\beta_l] \tag{34}$$

Here again, p is the blade that is impulsively accelerated, but now n corresponds to the number of the blade in the cascade for which the lift/moment is calculated.

Finally, this result can be convolved with any arbitrary motion of blade p to obtain the aerodynamic lift/moment on any blade n in the cascade. In general, all B blades may move with some arbitrary motion, so that a sum over p is required to obtain the most general expression for the lift/moment acting on blade n. Equations (8) and (9) can be modified accordingly

$$L_n(t) = \frac{1}{B}\sum_{p=1}^{B}\sum_{l=1}^{B}\int_0^t \bar{M}_{Lh}(t-\tau, \beta)\exp[j(p-n)\beta_l]\ddot{h}_p(\tau)\,d\tau + \frac{1}{B}\sum_{p=1}^{B}\sum_{l=1}^{B}\int_0^t \bar{M}_{L\alpha}(t-\tau, \beta)\exp[j(p-n)\beta_l]\ddot{\alpha}_p(\tau)\,d\tau \tag{35}$$

$$M_n(t) = \frac{1}{B}\sum_{p=1}^{B}\sum_{l=1}^{B}\int_0^t \bar{M}_{Mh}(t-\tau, \beta)\exp[j(p-n)\beta_l]\ddot{h}_p(\tau)\,d\tau + \frac{1}{B}\sum_{p=1}^{B}\sum_{l=1}^{B}\int_0^t \bar{M}_{M\alpha}(t-\tau, \beta)\exp[j(p-n)\beta_l]\ddot{\alpha}_p(\tau)\,d\tau \tag{36}$$

In summary, the cascade indicial function are found in terms of the constants α, ν, and μ in Eqs. (25) and (28). For any cascade executing arbitrary motion, the bending and pitching acceleration time history of each blade can be used as input to Eqs. (35) and (36) to obtain the aerodynamic lift and moment on each blade.

Results

Three FORTRAN programs are used for the model. The first program is LINSUB, which has been modified to output a table of aerodynamic coefficients at all possible interblade phase angles and over a range of reduced frequencies from −10 to 10. Although LINSUB can handle compressible flow, incompressible coefficients are obtained by setting the Mach number to a small value. The next program generates the cascade indicial functions in the form of a table of α, ν, and μ values. The last program reads in the indicial function coefficients and marches the equations of motion for the blades forward in time via a four-stage Runge–Kutta technique. Because the aerodynamic lift/moment calculations are computationally expensive, they are evaluated only once at each time step.

The equations of motion solved by the Runge–Kutta method are those for a two-dimensional airfoil section having two degrees of freedom, bending and torsion:

$$\bar{m}\ddot{h}_m + \bar{m}d\ddot{\alpha}_m + K_h h_m = L_m(t) \tag{37}$$

$$\bar{m}d\ddot{h}_m + \left(I_G + \bar{m}d^2\right)\ddot{\alpha}_m + K_\alpha \alpha_m = M_m(t) \tag{38}$$

for $m = 0, 1, \ldots, B$. Bending displacement and aerodynamic lift are positive up, whereas pitch angle an aerodynamic moment are positive nose down. The aerodynamic lift and moment are taken from Eqs. (35) and (36).

Example

The example case is a four-bladed rotor with 30-deg stagger and a spacing-to-chord ratio of 1. The mass and stiffness properties of the blades and the steady aerodynamic parameters are as follows. The blade parameters were chosen so that the in-vacuum bending and pitching natural frequencies are the same at 107.6 Hz, which corresponds to an in-vacuum reduced frequency of 0.90. Bending stiffness $K_h = 394600.0$ N/m^2, torsion stiffness $K_\alpha = 211.0$ N, moment of inertia $I_G = 0.000462$ kg · m, mass $\bar{m} = 0.8640$ kg/m, chord $c = 0.10$ m, $\overline{\text{e.a.}} = 0.00$, $d = 0.00$, density $\rho = 1.225$ kg/m, and velocity $U = 75.00$ m/s.

LINSUB Coefficients Curve Fit

A curve fit of the LINSUB coefficients over the range of reduced frequencies is required to generate the indicial functions. Figure 2 shows the lift due to bending as calculated from LINSUB for a 180-deg interblade phase angle. The associated curve fits using $I = 1$ and 2 in Eq. (23) are also shown, with the $I = 2$ result showing no visible difference between itself and the LINSUB result. The μ_1 value for both curve fits is 0.54, and μ_2 for the $I = 2$ case is 0.71.

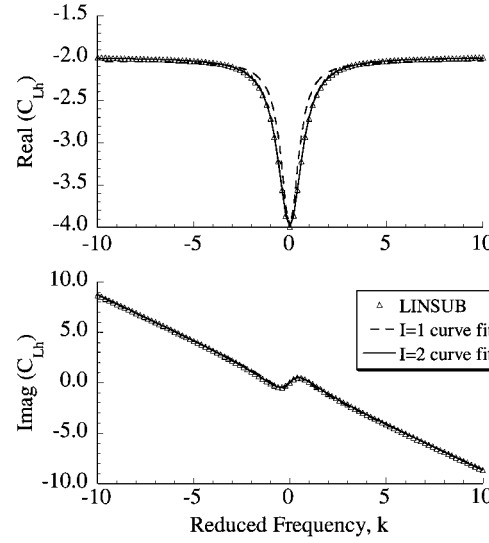

Fig. 2 Lift coefficient due to bending vs reduced frequency, 180-deg interblade phase.

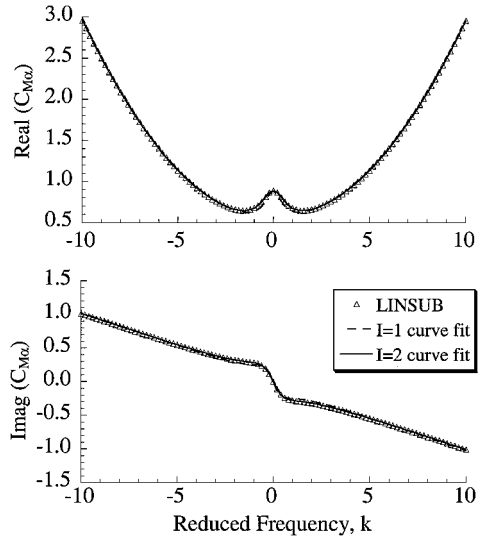

Fig. 3 Moment coefficient due to pitching vs reduced frequency, 180-deg interblade phase.

Figure 3 shows a similar plot for the moment due to bending at a 180-deg interblade phase angle. Figure 3 shows no visible difference between the both the $I = 1$ and 2 curve fit and the LINSUB result.

Verification via Comparison with LINSUB

The results from the model can be partially verified as follows. All of the blades are given initial conditions such that they oscillate in phase or with a 180-deg phase shift from blade to blade. Also, the aerodynamic coupling terms, that is, $\bar{M}_{L\alpha}$ and $\bar{M}_{Mh}$, are turned off to make two independent single-degree-of-freedom problems. The aerodynamic damping in the system can be represented by the exponential decay time constant τ, which for bending and torsion are

$$\tau_h|_{\text{time marching}} = \frac{t_2 - t_1}{\ell n[h(t_2)/h(t_1)]}$$

$$\tau_\alpha|_{\text{time marching}} = \frac{t_2 - t_1}{\ell n[\alpha(t_2)/\alpha(t_1)]} \tag{39}$$

where t_1 and t_2 are two times when the displacement reaches a peak.

The decay time constants based on the LINSUB aerodynamic coefficients are

$$\tau_h|_{\text{LINSUB}} = \frac{-2\bar{m}}{\rho U c\,\text{Re}(C_{Lh})} \qquad \tau_\alpha|_{\text{LINSUB}} = \frac{-2I_G\omega_\alpha}{\rho U^2 c^2\,\text{Im}(C_{M\alpha})} \tag{40}$$

Here ω_α is the dimensional in-air natural frequency in torsion. For a proper comparison, the natural frequency in air as calculated from the time-marching model is used for the frequency input to LINSUB.

The time-marching program was run for 0.03 s of simulation time, which corresponds to three cycles of oscillation. The peaks from the last two cycles were taken to evaluate the time constant. Two fully unsteady terms, that is, $I = 2$ in Eqs. (25) and (28), were used.

Table 1 shows a comparison of time constants for bending with zero interblade phase angle. For the case with zero initial velocity, the initial displacement was 2 mm for all blades. For the case with zero initial displacement, the initial velocity was 2 mm times the bending natural frequency for all blades. The reduced frequency in air was the same to within two significant digits of the in-vacuum natural frequency.

All simulations in Table 1 are from 0.0–0.03 s, with the number of iterations within this interval increased from 100 to 4000. At 500 iterations, the results are essentially converged to a value that is approximately 1% different from the LINSUB result. The kind of initial conditions, velocity or displacement, has no effect on the result except at low numbers of iterations.

Table 1 Damping constants for bending with 0-deg interblade phase angle

No. of iterations	$\tau_h\|_{\text{LINSUB}}$, s	$\tau_h\|_{\text{time marching}}$, s: Initial velocity = 0	$\tau_h\|_{\text{time marching}}$, s: Initial displacement = 0	CPU time, s
100	0.171	0.162	0.166	0.3
500	0.171	0.172	0.172	8.3
1000	0.171	0.172	0.172	34.1
2000	0.171	0.173	0.173	139.6
4000	0.171	0.173	0.173	555.9

Table 2 Damping constants for pitching with 0-deg interblade phase

No. of iterations	$\tau_\alpha\|_{\text{LINSUB}}$, s	$\tau_\alpha\|_{\text{time marching}}$, s: Initial velocity = 0	$\tau_\alpha\|_{\text{time marching}}$, s: Initial displacement = 0
100	0.102	0.0741	0.0743
500	0.102	0.0966	0.0966
1000	0.102	0.100	0.100
2000	0.102	0.102	0.102
4000	0.102	0.103	0.103

Table 3 Damping constants for bending and pitching with 180-deg interblade phase

No. of iterations	$\tau_x\|_{\text{LINSUB}}$, s	$\tau_x\|_{\text{time marching}}$, s: Initial velocity = 0	$\tau_x\|_{\text{time marching}}$, s: Initial displacement = 0
		Bending	
100	0.0670	0.0683	0.0672
500	0.0670	0.0674	0.0674
1000	0.0670	0.675	0.672
2000	0.0670	0.673	0.673
4000	0.0670	0.673	0.673
		Pitching	
100	0.0300	0.0232	0.0233
500	0.0300	0.0275	0.0276
1000	0.0300	0.0282	0.0282
2000	0.0300	0.0286	0.0286
4000	0.0300	0.0288	0.0288

A corresponding table for pitching with zero interblade phase angle is shown in Table 2. For the case with zero initial velocity, the initial displacement was 2 deg for all blades. For the case with zero initial displacement, the initial velocity was 2 deg times the pitching natural frequency. The reduced frequency in air was found to be 0.85, a decrease from the in-vacuum value of 0.90.

With 1000 iterations from 0.0 to 0.03 s, the results are essentially converged to a value approximately 2% different from the LINSUB result. The CPU times are not shown because they are the same as those in Table 1.

Table 3 summarizes the results for the 180-deg interblade phase angle cases. The amplitudes of the initial conditions are the same as those given earlier, with this amplitude now changing sign from blade to blade. The reduced frequency in air for bending was 0.90, essentially unchanged from in-vacuum reduced frequency. For pitching at a 180-deg interblade phase angle, the reduced frequency in air was 0.79.

For bending, with 2000 iterations from 0.0 to 0.03 s, the time-marching result is approximately 1% different from the LINSUB result. For pitching, the time constant for the time marching result is about 4% less than the LINSUB result at 4000 iterations.

These cases demonstrate that the theory developed herein is valid. Because the time-marching model uses a data file of aerodynamic coefficients from LINSUB, the results from the two models should be the same.

CPU Times

The CPU times in Table 1 are from an IBM RS/6000 model 580 workstation for the Runge–Kutta time-marching procedure only. The time required to generate the LINSUB coefficients for the baseline case at 101 reduced frequencies within the range $-10 < k < 10$ with 20 control points on the blade is 177 CPU s on the same workstation. This result scales linearly with the number of blades and is also largely affected by the spacing-to-chord ratio, with larger spacing-to-chord ratios requiring more time.

As shown in Table 1, the Runge–Kutta CPU times depend on the square of the number of iterations. This squared dependence is due to the convolution integral that is completely reevaluated at each time step. Further numerical experiments, not presented here, show that the Runge–Kutta CPU time depends on the square of the number of blades. This is expected because of the double summation over the number of blades in Eqs. (35) and (36). These two factors can drive CPU times up rapidly for large problems. Fortunately, making appropriate assumptions can decrease the CPU times significantly.

Note that the reevaluation of the convolution integral is necessary only for the fully unsteady terms in Eqs. (25) and (28). The quasi-steady and added-mass terms are such that the convolution integral can be reduced analytically to a simple dependence on displacement, velocity, or acceleration. Thus, most of the CPU time is consumed in evaluating the fully unsteady terms. Clearly, the advantage of using as few unsteady terms as possible is apparent. Two unsteady terms ($I = 2$) were used in all test cases herein, except where noted.

It is also possible to reduce the run times by only partially reevaluating the convolution integral at each time step. The idea is that, because the fully unsteady terms include an exponential decay, the terms at the beginning of the interval that have sufficiently decayed can be excluded from the integral. This exclusion is achieved by simply specifying the number of time steps NSAVE to include in the convolution integral evaluation.

When numerical experiments are performed, a measure is required to determine whether or not significant terms are being excluded from the convolution integral evaluation. Such a measure is

$$\underset{i}{\text{rms}} = \sqrt{\frac{1}{B}\sum_{l=1}^{B}\{\exp[-\mu_i(\text{NSAVE}-1)\Delta t]\}} \tag{41}$$

where Δt is the time step. This number gives the approximate magnitude of terms being neglected from the convolution integral.

Tables 4 and 5 give the results for different values of NSAVE for the case of a 180-deg interblade phase, zero initial velocity, 4000 time steps, and a final time of 0.03 s. Two fully unsteady terms were included in this case; thus, rms values for $i = 1$ and 2 are given.

Tables 4 and 5 indicate that Runge–Kutta CPU times can be decreased significantly without compromising the accuracy of the results. The numbers in the last column show an approximate order of magnitude decrease from the first term to the last term included in the convolution integral. It seems reasonable from these results that the $\log_{10}(\text{rms}_i^{-1})$ values be kept larger 1.0 to assure a good solution.

General Cases

In the preceding cases, the aerodynamic coupling terms $\bar{M}_{L\alpha}$ and $\bar{M}_{Mh}$ were calculated so that CPU times are accurate. However, their effect was neglected so that a comparison with LINSUB could be made. Now consider cases where the effect of the coupling terms is included.

Table 4 Damping constants for bending with 180-deg interblade phase angle for differing NSAVE

NSAVE	LINSUB τ_h, s	Time marching τ_h, s	CPU time, s	$\log_{10}(\text{rms}_i^{-1})$ $i = 1/i = 2$
100	0.0670	0.0496	19.4	0.13/0.17
500	0.0670	0.0682	124.3	0.66/1.5
1000	0.0670	0.0675	237.6	1.3/1.5
2000	0.0670	0.0673	410.8	2.6/2.9
4000	0.0670	0.0673	555.9	5.3/5.6

Table 5 Damping constants for pitching with 180-deg interblade phase angle for differing NSAVE

NSAVE	LINSUB τ_α, s	Time marching τ_α, s	CPU time, s	$\log_{10}(\text{rms}_i^{-1})$ $i = 1/i = 2$
100	0.0300	0.0174	19.4	0.13/0.17
500	0.0300	0.0280	124.3	0.66/1.5
1000	0.0300	0.0290	237.6	1.3/1.5
2000	0.0300	0.0288	410.8	2.6/2.9
4000	0.0300	0.0288	555.9	5.3/5.6

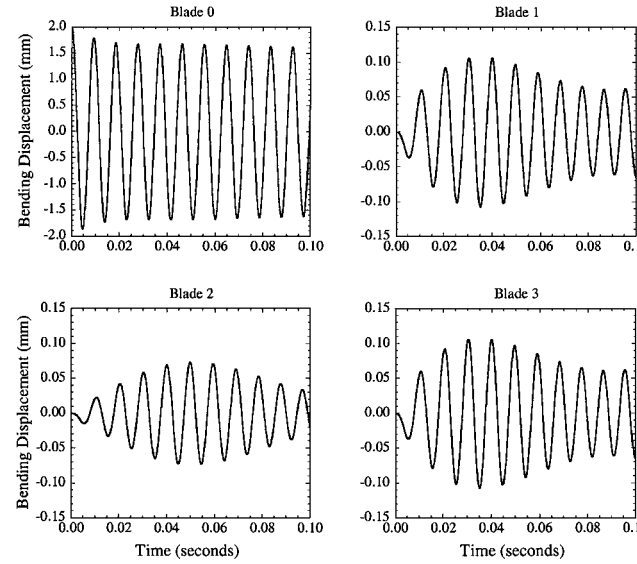

Fig. 4 Bending time histories for four-bladed rotor with 0-deg stagger, *s/c* = 1.0.

Stagger of 0 deg, s/c = 1.0

The same basic configuration of four blades with a spacing-to-chord ratio of 1.0 is considered, except now the stagger has been set to zero.

For initial conditions, blade $m = 0$ is displaced by 2 mm. All of the other displacements and velocities are set equal to zero. This case was run for 0.10 s. There were 4000 time steps used, with 500 terms included in the convolution integral. With NSAVE = 500, the $\log_{10}(\text{rms}_i^{-1})$ values were greater than 2.0. The total CPU time required was 124.3 s.

Figure 4 shows the bending displacement time histories for the four blades. The motion of blade 0 produces an aerodynamic force on the other blades, causing them to vibrate. For this case, with 0 deg of stagger, the motion of blades 1 and 3 is the same due to symmetry. Note that the scale for blade 0 is much larger than that for the other blades because blade 0 vibrates with the largest amplitude, as expected.

Figure 5 shows the pitching time histories for the four blades. Although there was no initial pitching displacement, the aerodynamic coupling term $\bar{M}_{Mh}$ produces a moment on the blades. Note again that the scale for blade 0 is larger than that of the other blades.

Stagger of 30 deg, s/c = 1.0

Next, the stagger angle was changed from 0 to 30 deg. All other conditions, including the initial conditions, are the same. Figures 6 and 7 show the bending and pitching time histories of the four blades. In contrast to the 0-deg stagger case, the motion of blades 1 and 3 is not the same due to the antisymmetry introduced by the nonzero stagger.

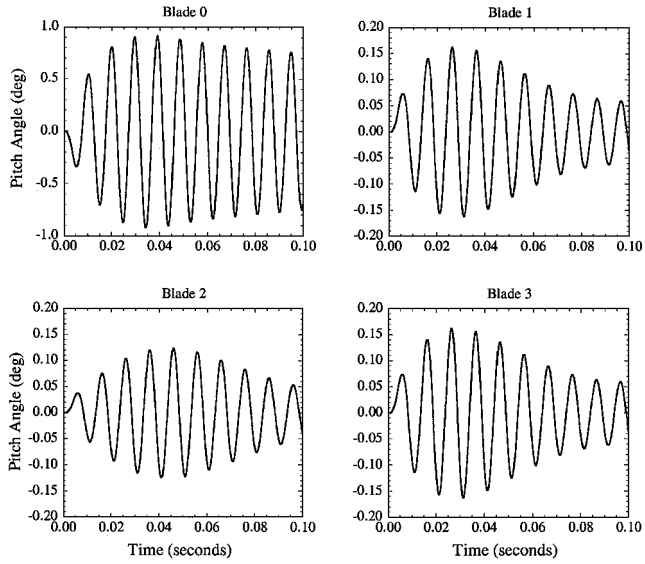

Fig. 5 Pitching time histories for four-bladed rotor with 0-deg stagger, s/c = 1.0.

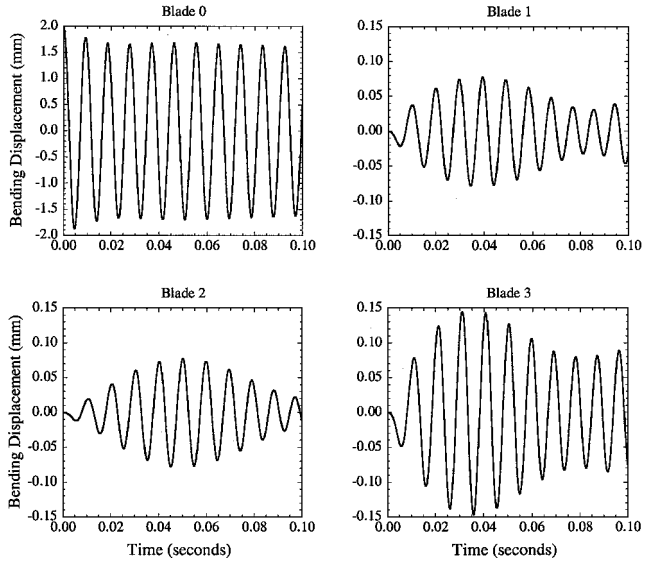

Fig. 6 Bending time histories for four-bladed rotor with 30-deg stagger, s/c = 1.0.

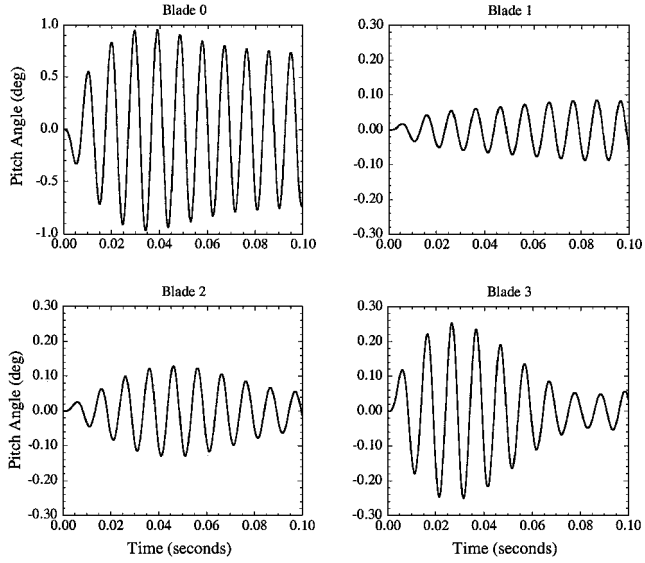

Fig. 7 Pitching time histories for four-bladed rotor with 30-deg stagger, s/c = 1.0.

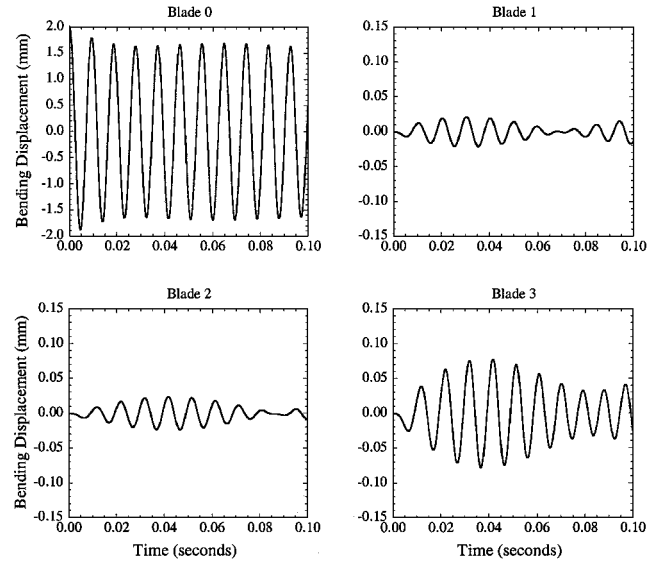

Fig. 8 Bending time histories for four-bladed rotor with 30-deg stagger, s/c = 2.0.

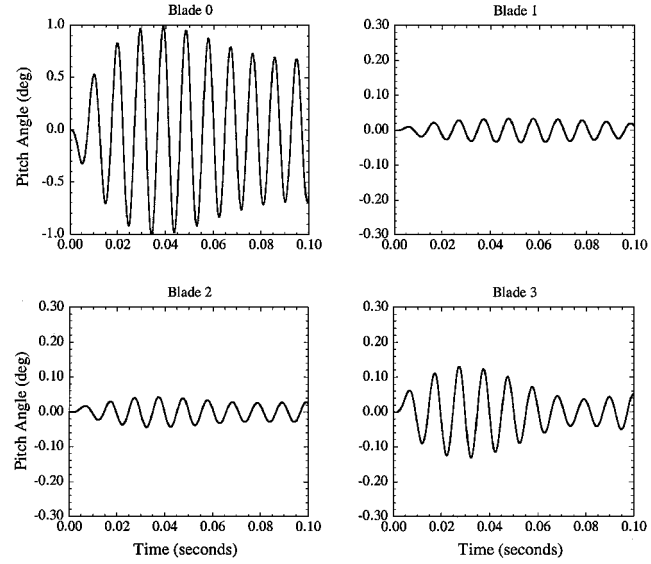

Fig. 9 Pitching time histories for four-bladed rotor with 30-deg stagger, s/c = 2.0.

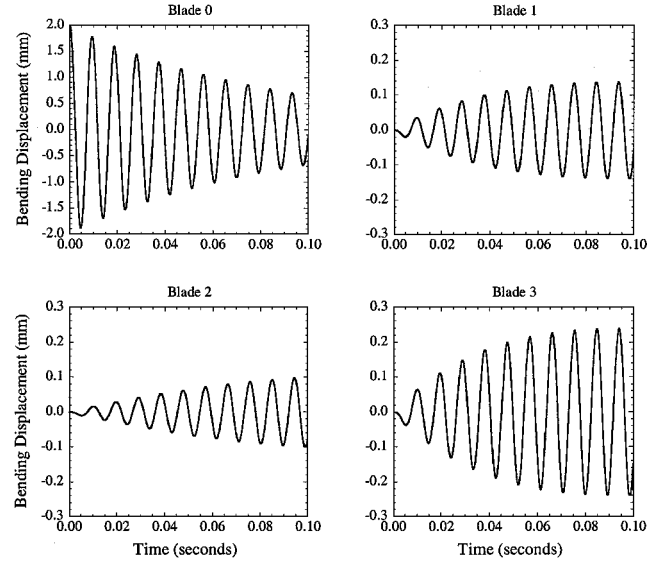

Fig. 10 Bending time histories for four-bladed rotor with 30-deg stagger, s/c = 1.0, and in-vacuum torsion natural frequency of 215.1 Hz.

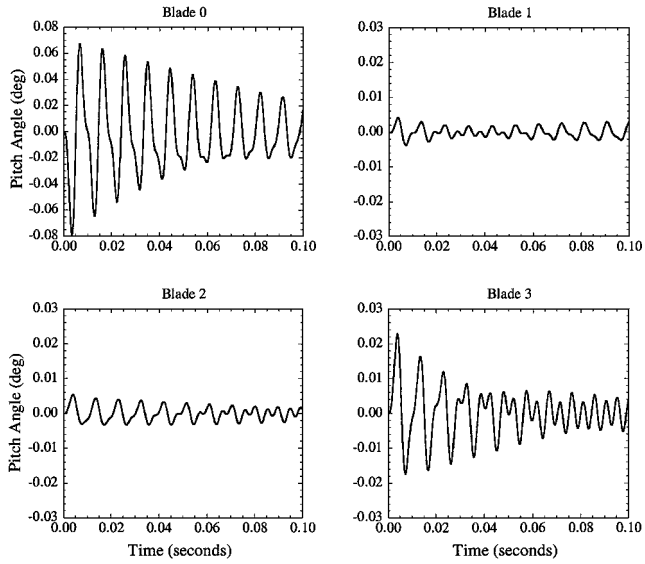

Fig. 11 Pitching time histories for four-bladed rotor with 30-deg stagger, *s/c* = 1.0, and in-vacuum torsion natural frequency of 215.1 Hz.

Stagger of 30 deg, s/c = 2.0

Next, the spacing-to-chordratio was increased to 2.0. To have the same magnitude of error in the curve fit of LINSUB coefficients, three unsteady terms ($I = 3$) were used in Eqs. (23) and (26). This is consistent with Mengle's[3] finding that more terms are needed as the spacing increases. The CPU time required was 187.2 s. The results are shown in Figs. 8 and 9. As expected, the larger spacing decreases the aerodynamic interaction from one blade to the next. The blade 0 response is essentially the same as before, but blades 1 through 3 are seen to have much lower amplitudes as compared to the $s/c = 1.0$ case.

Torsion In-Vacuum Frequency Doubled

In the final case, the 30-deg stagger, $s/c = 1.0$ configuration is revisited, except that now the torsion natural frequency has been doubled via a quadrupling of the torsion stiffness. Blade $m = 0$ is initially displaced by 2 mm, with the resulting blade vibration time histories shown in Figs. 10 and 11. When Figs. 10 and 6 are compared, the larger decay rate shows that energy is more quickly extracted from blade 0 because the torsion and bending modes can no longer easily exchange energy, these now having differing natural frequencies. A power spectrum (not shown) of Fig. 11 indicates that there are two frequencies present in the response of all blades, the lower frequency at the bending natural frequency and the higher at the torsion natural frequency. The lower frequency is due to an external moment forcing caused by the bending motion of the blades, whereas the higher frequency is the homogeneous response. When Figs. 11 and 7 are compared, the doubling of the torsion natural frequency has substantially reduced the pitching amplitude.

Summary

A linearized unsteady incompressible aerodynamic model for airfoil cascades was developed that is not restricted to harmonic motion at a constant interblade phase angle. The method presents designers with a new tool for modeling unsteady aerodynamics for a bladed disk environment wherein the blades have different oscillation frequencies and amplitudes. This was accomplished by starting with the unsteady aerodynamic coefficients generated by LINSUB, a semi-analytic unsteady cascade aerodynamics code. An inverse Fourier transform is performed to predict the unsteady aerodynamic forces on the airfoils due to an impulsive acceleration. This result, termed the cascade indicial function, is then convolved with the arbitrary motion of the blades to obtain the unsteady aerodynamic forces on the airfoils in the time domain.

The aerodynamic damping predicted by the time-domain model was shown to compare well to LINSUB results when the interblade phase angle is constant. Results demonstrating the model's ability to predict unsteady aerodynamics for a cascade with arbitrary airfoil motion were also presented.

Although LINSUB aerodynamic coefficients were used herein, the method can use aerodynamic coefficients from more advance flow models, as long as these coefficients function as constants of proportionality between the aerodynamic modal force and airfoil modal displacement or velocity.

Acknowledgments

This research was sponsored, in part, by the Air Force Office of Scientific Research. This support is most gratefully acknowledged.

References

[1] Smith, S. N., "Discrete Frequency Sound Generation in Axial Flow Turbomachines," Engineering Dept., Cambridge Univ., Cambridge, England, U.K., Repts. and Memoranda 3709, March 1972.

[2] Verdon, J. M., and Hall, K. C., "Development of a Linearized Unsteady Aerodynamic Analysis for Cascade Gust Response Predictions," NASA CR 4308, 1990.

[3] Mengle, V. G., "Unsteady Aerodynamic Response of Cascade and Turborotors," Ph.D. Dissertation, Aerospace Engineering Dept., Cornell Univ., Ithaca, NY, May 1984.